Simulation and Analysis of Switched Capacitor dc-dc Converters for Use in Battery Electric Vehicles

Yue Cao, Zichao Ye[1], *Student Member*, *IEEE*

***Abstract*—This paper presents a switched capacitor dc-dc converter based electric drive system for battery electric vehicles. The main idea is to replace the traditional IGBT boost converter by modular battery cell tied MOSFET switched capacitor converters. The system topology is presented, including the drive train architecture. The modeling approach for each electrical component, including the battery set, dc-dc and dc-ac converters, ac machines, and their control is discussed. Upon successful simulations, various efficiency analyses are performed. Finally, potential hardware implementation, including economic and spacing constraints, is discussed.**

***Index Terms*—Switched capacitor dc-dc converters, electric vehicles, ac drives, lithium-ion batteries**

I. Introduction

Switched capacitor (SC) converters have gained in popularity in recent years, and are being applied at increasing power levels [l]. SC converters are significantly different from power converters that use bulky magnetic energy storage elements. Fundamentally, SC converters have equivalent resistance that determines their performance, and is generally much higher than the output impedance of a converter that uses inductors to store energy [2-3]. With capacitors as only energy storage elements in SC, design and selection of capacitor technology is particularly important for high power converters [4].

Battery packs in existing battery electric vehicles (BEV) require a boost converter for batteries to connect with the dc bus before powering the ac drive and machine. The battery packs consist of many single-cell lithium-ion batteries, usually 3.2-4.0 V each depending on their state of charge (SOC). They are connected in series to form a 300-400 V source, which is boosted to around 700 V for the dc bus. [5] Instead of one main bulky IGBT based converter between the battery packs and the dc bus, battery cell attached modular SC converters, based on MOSFET, can be proposed. All the SC converters are connected in series at the output and form a 600-800 V dc bus directly. In existing power train topologies, the dc bus is regulated to a fixed voltage by the boost converter. Since the conversion ratio for a SC converter is fixed by its circuit topology, the output of all the SC converters will vary depending on the battery SOC. However, a design can be selected to ensure a minimum dc bus voltage, and for higher voltages, the ac drive can be controlled to operate normally.

Possible advantages for modular SC converters in the BEV application include reduced volume consumption, improved thermal flows, flexible structures, improved battery cells balance, and increased reliability/fault bypass, etc. However, many other factors are unknown, such as the proposed system's feasibility, efficiency, cost, thermal effect, reliability, and also its impact on the motor drive due to floating voltages. This project is therefore to design and simulate such a system and compare it with an existing system. A more comprehensive analysis may also include variations in system topology or system operation points. Note that in this paper, the focus is at system level simulation and not at component level design.

II. BEV System Topology with SC Converters

Figure 1 shows the proposed system: the battery connects to the dc bus through a dc-dc converter; then a dc-ac inverter drives an ac induction machine. It is most important to observe the power and efficiency in each subsystem.

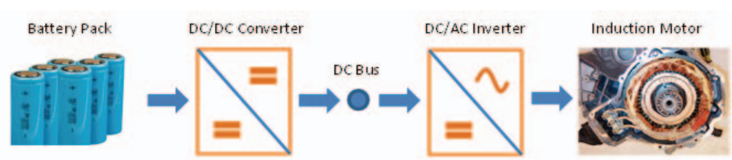

Figure 1. Battery electric vehicle power system structure

The traditional power system utilizes a 300-400 V battery pack and a main dc-dc converter. In the proposed system, a single cell battery can form a module with a SC converter, and the modules connect in series to form a dc bus. This is illustrated in Figure 2 and Figure 3, respectively. Note that there must be multiple columns of modules in parallel so that the total output current meets the ac drive demand while at the same time each battery cell does not exceed its recommended discharge current rating (usually 1C, e.g., in a 2.2 A-h battery it is 2.2 A).

Figure 2. A single battery cell and a SC converter formed power module

[1]Yue Cao and Zichao Ye are with the Department of Electrical and Computer Engineering, University of Illinois, Urbana, IL 61801, USA (email: yuecao2@illinois.edu, zye4@illinois.edu).

978-1-4799-7949-3/15/$31.00 ©2015 IEEE

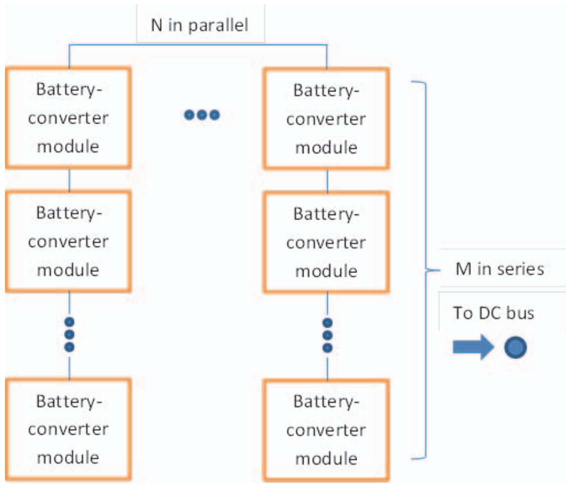

Figure 3. Series and parallel structure for proposed modules

III. Modeling

A 1:2 step-up SC converter is chosen for the simulation study. However, a 1:3 (or 1:N) boost SC converter may be also used to reduce the number of series connected battery cells while increasing the number of passive elements in the SC converter. The 1:2 SC converter topology is shown in Figure 4. Note that both Q1 switches are controlled by the same signal, and both Q2 switches are controlled by the complement. The signal is simply 50% duty ratio, thus making the control less complicated compared to the boost converter with closed loop feedback.

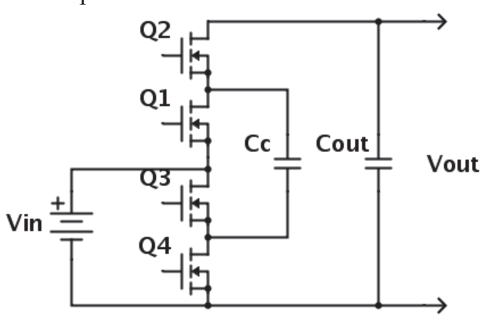

Figure 4. A 1:2 boost SC converter circuit topology

The battery model is based on the circuit in Figure 5, in which voltage source, resistors and capacitors depend nonlinearly on the battery's SOC:

$$\ln(V,C,R) = a_0 + a_1 \ln(SOC) + \ldots + a_6 \ln^6(SOC) = \sum_{k=0}^{6} a_k \ln^k(SOC) \tag{1}$$

The coefficients in (1) found in [7] are from curve fitting of experimental data of V, C, and R versus SOC. SOC is modeled as in [6] as

$$SOC(t) = SOC_{initial} + \int_0^t f_1[i_{charge}(t)] \times i_{charge}(t)dt + \int_0^t f_2[i_{discharge}(t)] \times i_{discharge}(t)dt \tag{2}$$

Functions f_1 and f_2 are look-up tables from current testing [6]. Single-cell data (current, SOC) were extracted from measurements of the Panasonic CGR18650A 3.7 V, 2.2 A-h Li-ion batteries. The battery terminal voltage is then calculated as

$$V_t = V_{oc} - I_c(R_{series} + R_{ts} \,||\, \frac{1}{sC_{ts}} + R_{tm} \,||\, \frac{1}{sC_{tm}} + R_{th} \,||\, \frac{1}{sC_{th}}) \tag{3}$$

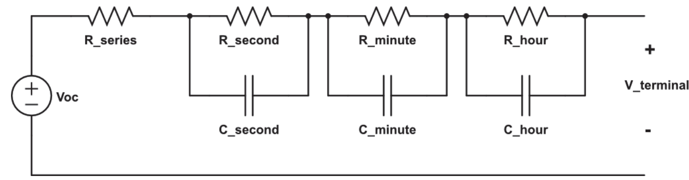

Figure 5. Lithium-ion battery model circuit

Notice that the model includes explicit dynamics on time scales of seconds, minutes, and hours.

The induction machine (IM) is modeled as differential equations [8]

$$\begin{aligned}
V_{qs} &= R_s i_{qs} + d\varphi_{qs}/dt + \omega\varphi_{qs} \\
V_{ds} &= R_s i_{ds} + d\varphi_{ds}/dt + \omega\varphi_{ds} \\
V'_{qr} &= R'_r i'_{qr} + d\varphi'_{qr}/dt + (\omega-\omega_r)\varphi'_{dr} \\
V'_{dr} &= R'_r i'_{dr} + d\varphi'_{dr}/dt + (\omega-\omega_r)\varphi'_{qr} \\
T_e &= 1.5p(\varphi_{ds} i_{qs} - \varphi_{qs} i_{ds}) \\
d\omega_m/dt &= (1/2H)(T_e - F\omega_m - T_m)
\end{aligned} \tag{4}$$

A scalar volts-per-hertz (V/f) control (Figure 6) is implemented in the IM drive (Figure 7), which can be controlled to respond robustly to a wide range of torque and speed commands.

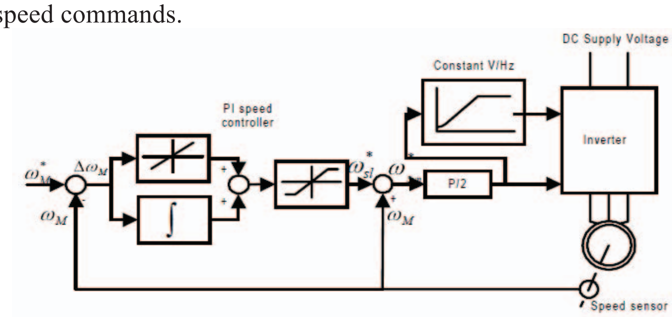

Figure 6. Induction machine V/f closed-loop control diagram

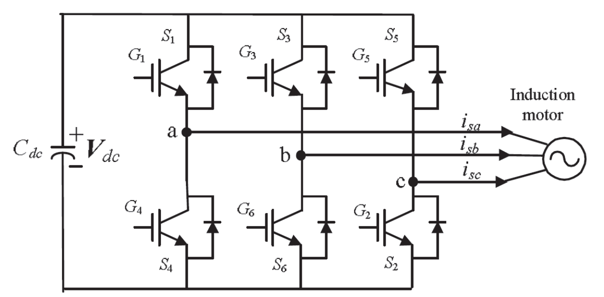

Figure 7. dc-ac inverter circuit tied to the ac motor

IV. Simulation Setup

A comprehensive simulation must be run for the integrated system. It is important to evaluate performance under real-life scenarios, which include the variations in battery SOC, output powers, etc. Each of the system components mentioned in Section III needs to be designed with realistic requirements. The goal is to power a 460 V ac induction machine up to about 100 kW (134 HP) for automotive applications. For this simulation study, 2-10 kW, 1/10 scale, will be conducted. More power requires more parallel battery branches, thus significantly slowing down the simulation speed. However, for the efficiency study this power level is still deemed valid because the power flowing through each SC converter module is unchanged. Similarly for the dc-ac inverter, higher power simply means more IGBT's in parallel, which does not have major impact on single devices' efficiency.

The 460 V ac induction machine requires a minimum 650 V dc bus. In order to achieve this voltage level, 100 Panasonic lithium-ion batteries need to be connected in series. At least 5 parallel branches need to be formed to produce a nominal power of 4.3 kW when 1C of current is drawn. A 2.3C current will be produced when 10 kW is required. This is under the battery output capability, since the peak power is only demanded for a short period of time.

The most focused design for this project is for the SC converter. Two major devices need to be chosen, i.e., the charging capacitor, C_c, and the output capacitor, C_{out}. For C_c, it is part of the converter's output impedance, and this impedance can be determined in terms of just the charge multiplier components [9]:

$$R_{SSL} = \sum_{capacitors} \frac{(a_{c,i})^2}{C_i f_{sw}} \tag{5}$$

$$R_{FSL} = 2 \sum_{switches} R_i (a_{r,i})^2 \tag{6}$$

A good approximated operation point based on (5) and (6) is therefore

$$\frac{1}{R_{eq} C_c} = 2\pi f_{sw} \tag{7}$$

For this particular application, 8 V 12 A (~5C) MOSFET's are used, which have R_{ds} of 9.4 mΩ each. A 100 kHz switching frequency is selected. Hence C_c is calculated to be about 80 μF. C_{out} is calculated based on the following

$$C_{out} = \frac{D I_{out}}{f_{sw} \Delta V_{out}} \tag{8}$$

It is desired to have 1.1 A of continuous output current, duty ratio of 50%, and the voltage ripple of 0.05 V for each SC converter module. Hence C_{out} is found to be 110 μF. Note for accurate simulation, ESR's are also included.

For the conventional dc-dc boost converter, 1200 V 50 A IGBT's are used. A 10 kHz switching frequency is selected. From similar calculations as the above, a 200 μH input inductor and a 1000 μF output capacitor are required.

The dc-ac inverter and the ac induction machine are held the same for both SC converter and conventional boost converter topologies. The cost is the same for both scenarios, but the efficiencies may be different, since the dc bus voltage for the SC converter case is floating and varying modulation indexes are needed.

V. Simulation Results

To demonstrate the capabilities of the integrated system, a transient response is simulated in the MATLAB/Simulink environment. A transient response is needed because higher currents are drawn at the starting of the machine, thus putting more stress on the battery and SC converters. The transient response eventually settles to stability and also illustrates the steady state operation.

Figure 8 shows the acceleration of the induction machine from 0 to about 187 rad/sec (1780 RPM) within one second. The figure also shows the stator current, which is also the current out of the dc-ac inverter. A steady-state torque of about 20 Nm indicates the output power is about 3750 W. This operating condition is specifically chosen such that the output current from the battery cell is about 1C (2.2 A), which results its nominal operation. The machine runs without a problem, meaning that the batteries and SC converters can handle such accelerating transients. One thing worth mentioning is that the torque has higher ripples compared to that from the traditional boost. This may be compensated by a more advanced ac drive control rather than the V/f control.

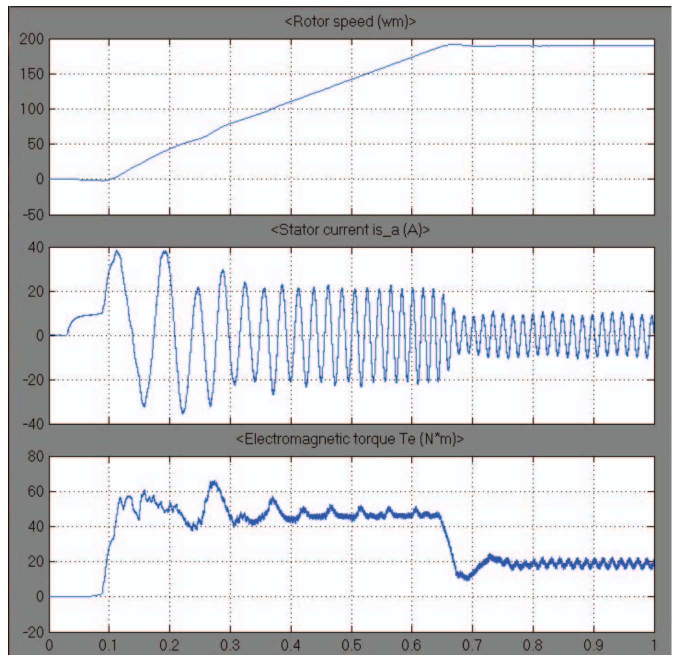

Figure 8. Induction machine speed, current, and torque during acceleration

Figure 9 shows the input and output voltages of the dc-ac inverter as well as the modulation index required to operate the induction machine. Notice that the dc bus voltage is well below 760 V (steady-state) at the beginning. This is because the current flowing through the batteries is well above the nominal current, thus pulling down their terminal voltage.

Figure 10 shows the output capacitor and the charging capacitor voltages for each battery-converter module. These waveforms are similar to that of the dc-bus voltage. Looking closer, it can be observed that the output voltage ripple is about 0.05 V, which is true to the designed value in Section IV.

Figure 11 correctly demonstrates each battery cell SOC, voltage, and current during the transients. The voltage level is within the reasonable range for a fully charged battery, and the current level eventually settles down to about 2.2 A, which is the nominal operating condition designed from above.

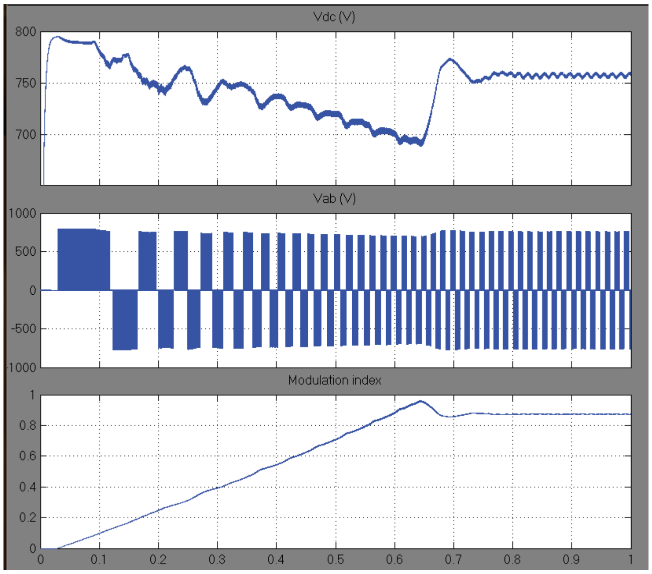

Figure 9. dc-ac inverter input and output voltages and modulation index

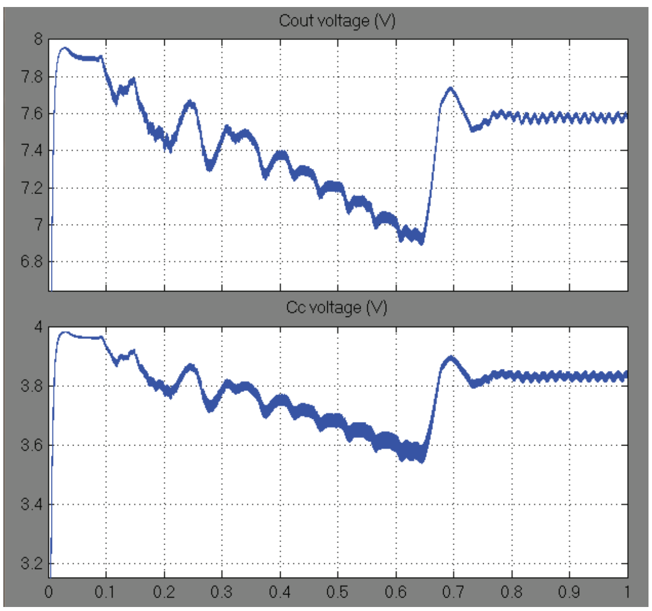

Figure 10. Output and charging capacitors voltages

VI. ANALYSIS – EFFICIENCY

The simulation has successfully completed, and the results are reasonable based on previous experiences. When talking about efficiencies, for this application, we are mostly interested in the system level efficiency. From the transient simulations in Section V, the overall system efficiency can be found for both SC converter and boost converter topologies. For the SC converter, the number is 82.8%, and for the boost converter, the number is 78.6%, about 4% lower. This is significant considering the power level in this context. Note that this simulation run is only for this particular operating condition, i.e., 1.0 battery SOC and 2.2 A battery current, which determine the system's voltage and load, respectively. However, in real life the battery SOC and output current vary depending on the drive cycle. Another steady-state efficiency analysis must be performed in order to compare the efficiencies under different scenarios. Because the only difference between the SC converter and boost converter system topologies is at the dc-dc conversion, efficiencies at the batteries, dc-ac inverter, and the induction machine can be deemed as equivalent between the two system configurations.

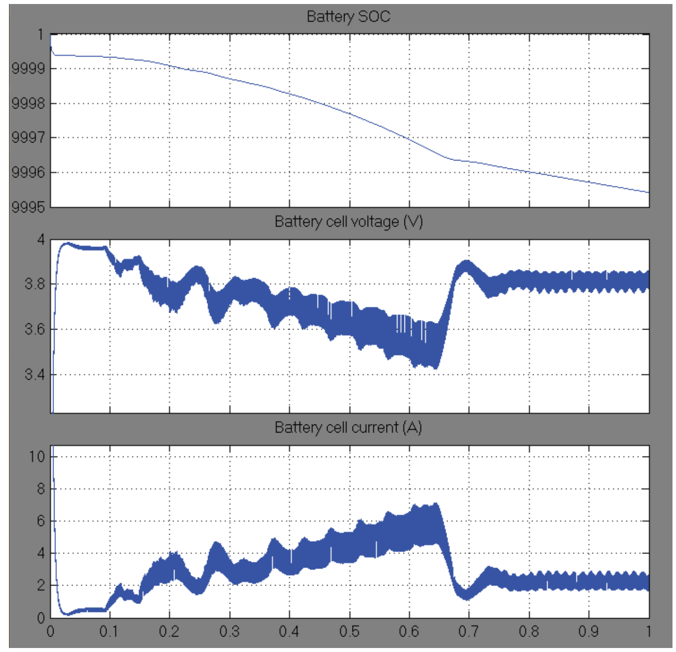

Figure 11. Battery cell SOC, voltage, and output current

Table 1 presents the dc-dc conversion efficiencies when battery SOC and output current change. The nominal output current is about 2.2 A, and the SOC is recommended to be at least 0.5 for maximum battery life. From the table, it can be noticed that the SC converter efficiency first increases and then decreases when the output current increases. However, it appears that the battery SOC has little impact on the converter efficiency. The results indicate that the SC converter is better performed when the load is light. This is ideal because most of the time the car is running at light load except when acceleration or hill climbing is needed. We can also learn that the SC converter can perform equally well even when the battery SOC is low.

Table 2 is a similar study for the traditional boost converter. It can be noticed that the boost converter works more efficiently when there are heavier loads. The battery SOC also has some degree of impact on the efficiency: lower SOC's result in lower dc-dc conversion ratio.

Figure 12 shows the efficiencies from the two converters versus battery output currents when the SOC is 1.0. It is clear that SC converter outperforms the boost converter under light loads. Only after about 1.5C current does the boost converter become more efficient.

Table 1. SC converter efficiency at different battery SOCs and output currents

	1.0 A out	2.0 A out	3.0 A out	4.0 A out	5.0 A out
1.0 SOC	93.2%	96.3%	93.6%	89.8%	87.2%
0.9 SOC	93.3%	96.3%	93.6%	89.8%	87.2%
0.8 SOC	93.3%	96.4%	93.7%	89.9%	87.3%
0.7 SOC	93.4%	96.4%	93.7%	89.9%	87.3%
0.6 SOC	93.4%	96.4%	93.7%	89.9%	87.3%
0.5 SOC	93.3%	96.3%	93.6%	89.8%	87.2%

Table 2. Boost converter efficiency at different battery SOCs and currents

	1.0 A out	2.0 A out	3.0 A out	4.0 A out	5.0 A out
1.0 SOC	81.6%	89.5%	90.4%	92.1%	92.7%
0.9 SOC	80.7%	88.9%	90.5%	91.9%	92.5%
0.8 SOC	80.9%	86.4%	90.5%	91.9%	91.6%
0.7 SOC	81.8%	87.3%	90.7%	91.9%	91.6%
0.6 SOC	77.0%	87.2%	90.5%	90.8%	91.6%
0.5 SOC	78.4%	87.5%	92.6%	90.9%	91.6%

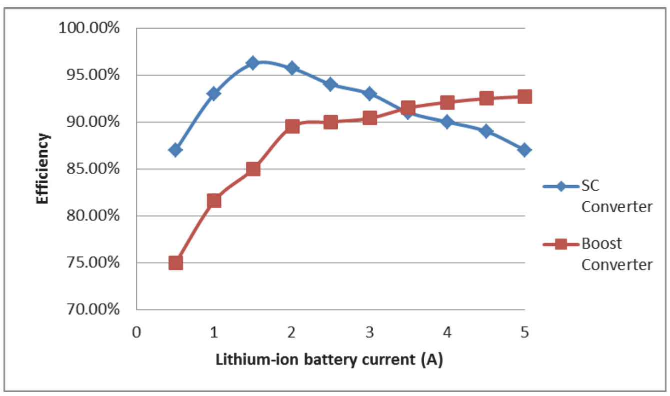

Figure 12. SC and boost converters efficiencies versus battery output currents

VII. Analysis – Cost and Dimension

One major concern to the industry is the cost. It is often observed that a superior design is turned down from production because of the cost. Therefore, it is important to have an estimate of the potential SC converter cost versus the traditional boost converter. The estimate in Table 3 [10] includes most passive and semiconductor devices, thermal and protection hardware, and miscellaneous substances. Note that this estimate is for the specific scenario described in Section IV, and also that this includes only the front end, i.e., the dc-dc conversion part, but not the motor drive and machine. It is assumed that heat sinks and cases are not required for the SC converters because they are tied together with the batteries and can dissipate heat through natural conditions.

From the table, it can be seen that the SC converter's power electronics costs about $500 more for each traction unit. However, the SC converters are overall more efficient as analyzed from Section VI. The energy saved will eventually make the investment break-even. In addition, they are modulized, which provides more flexibility and reliability in case of faults.

Table 3. Hardware cost comparison between SC and boost converters

Device	SC converter		Boost converter	
	Unit cost ($) × # of units	Total cost ($)	Unit cost ($) × # of units	Total cost ($)
MOSFET	0.232×2000	464	0	0
IGBT/Diode	0	0	49.83×2	97.66
Capacitor	0.379×1000	379	114.62×1	114.62
Inductor	0	0	30.55×1	30.55
Heat sink	0	0	57.61×1	57.61
Case	0	0	54.16×1	54.16
Total	$843		$354.6	

Another concern to the engineers is whether there is enough space to assemble everything. Figure 13 presents a visual of the expected sizes for a traditional boost converter, from Toyota Prius [11], and a typical SC converter [12]. Even though there are hundreds of SC converters versus only one boost, the SC converters can be integrated with the batteries and their battery management system. The space saved from the absence of the boost can be used to store more batteries or other energy sources.

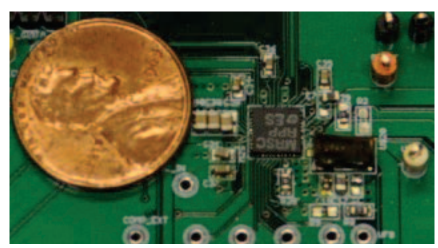

Figure 13. Traditional dc-dc converter used in hybrid electric vehicles (top) and single SC converter to be used with battery (bottom)

VIII. Conclusion and Future Work

A battery electric vehicle traction system utilizing lithium-ion batteries, switched capacitor converters, a dc-ac inverter and an ac induction machine has been modeled and simulated under various operating conditions, including transient and steady-state analysis. A similar system with a traditional boost converter is also simulated for comparison purposes. The results show that the SC converter topology yields higher efficiencies under nominal or light loads, whereas the boost converter topology is more efficient at heavy loads. The results also show that the battery SOC has little impact on SC converter efficiencies. From the economic perspective, the SC converter costs about double. However, by converting energy more efficiently, this topology is expected to save money in the long run. The SC converter also reduces hardware space required, hence leaving more room for more energy storage.

The simulation work in this paper provides reasonable results, which may be useful for future research and development in the field of battery-SC converter based ac motor drives for automotive applications. It will be desired to have hardware implementation, possibly on a smaller scale due to lab work constraint, to prove the relevant performance from this simulation. A more comprehensive simulation at a full 100 kW or even a few hundred kW scale is desired to present more insightful information. Regenerative braking/battery charging can be also simulated and discussed at a system's level. In addition, a 1:3 SC converter, for example, may be used to save some battery cells, with possibly a sacrifice of efficiency on the other hand. Thermal and reliability issues are not presented in this paper due to the complex nature of this project and the knowledge limitation of the author.

References

[1] A. Ioinovici, "Switched-capacitor power electronics circuits," *IEEE Circuits and Systems Magazine*, vol. 1, issue 3, pp. 37-42, 2001.

[2] J. W. Kimball and P. T. Krein, "Analysis and design of switched capacitor converters," in *Proc. IEEE Applied Power Electronics Conf.*, 2005, pp. 1473-1477.

[3] Y. Lei and R.C.N. Pilawa-Podgurski, "Soft-charging operation of switched-capacitor DC-DC converters with an inductive load," in *Proc. IEEE Applied Power Electronics Conf.*, 2014, pp. 2112-2119.

[4] F. Z. Peng, F. Zhang, Z. Qian, "A magnetic-less DC-DC converter for dual-voltage automotive systems," *IEEE Trans. on Industry Applications*, vol. 39, pp. 511-518, March-April 2003.

[5] B. Bural, et al., "An experimental comparison of different topologies for fuel-cell, battery and ultra-capacitor in electric vehicle," in *Proc. IEEE National Conf. on Electrical, Electronics, and Computer Engineering*, 2010, pp. 46-52.

[6] R. C. Kroeze and P. T. Krein, "Electrical battery model for use in dynamic electric vehicle simulations," in *Proc. IEEE Power Electronics Specialists Conf.*, 2008, pp. 1336-1342.

[7] Y. Cao and P. T. Krein, "An average modeling approach for mobile refrigeration hybrid power systems with improved battery simulation," in *Proc. IEEE Transportation Electrification Conf.*, 2013, pp. 1-6.

[8] P. C. Krause, O. Wasynczuk, and S. D. Sudhoff, *Analysis of Electric Machinery and Drive Systems*, 2nd ed. Edison, NJ: Wiley-IEEE Press, 2002, pp. 525-556.

[9] M. Seeman and S. R. Sanders, "Analysis and optimization of switched-capacitor dc-dc converters," *IEEE Trans. on Power Electronics*, vol. 23, no. 2, pp. 841-851, March 2008.

[10] [Online]. Available: http://www.digikey.com

[11] [Online]. Available: http://www.toyota- industries.com/csr/environment/product/erectoronic_01.html

[12] R.C.N. Pilawa-Podgurski and D.J. Perreault, "Merged two-stage power converter with soft charging switched-capacitor stage in 180 nm CMOS," *IEEE Journal of Solid-State Circuits*, vol. 47, no. 7, pp. 1557-1567, 2012.